



## **The Effect of Carbon Nanotube on Improving Catalytic G-quadruplex Sensing Properties**

**Fahimeh Otovat<sup>1</sup>, Mohammad Reza Bozorgmehr<sup>2, \*</sup>, Ali Mahmoudi<sup>1</sup>, Ali Morsali<sup>2</sup>**

<sup>1</sup>*Faculty of Chemistry, Islamic Azad University, North Tehran Branch, Hakimiyyeh, Tehran, Iran*

<sup>2</sup>*Department of Chemistry, Mashhad Branch, Islamic Azad University, Mashhad, Iran*

*(Received 10 Feb. 2023; Final revised received 15 May 2023)*

---

### **Abstract**

In the use of G-quadruplex as DNAzyme, the background signal corresponding to Hemin is high. Therefore, it limits the application of DNAzyme. If carbon nanotubes are added to the system containing G-quadruplex and Hemin, this problem will be solved. However, the mechanism of the nanotube effect on DNAzyme is not known. In this work, molecular dynamics simulation was used to clarify this mechanism. The interaction between G-quadruplex and Hemin was simulated in the presence and absence of carbon nanotubes. The calculated distance between the center of mass of G-quadruplex and Hemin during the simulation time shows that the nanotube increases the affinity of hemin to G-quadruplex. Also, the calculation of the conformational factor of the G-quadruplex residues shows that Hemin is bonded to the G-quadruplex from the top and side. The obtained results are in good agreement with the available experimental evidence.

**Keywords:** Biosensor, Signal, Conformational factor, DNA, Enzyme.

---

*\*Corresponding author: Mohammad Reza Bozorgmehr, Department of Chemistry, Mashhad Branch, Islamic Azad University, Mashhad, Iran. Email: bozorgmehr@mshdiau.ac.ir (mr\_bozorgmehr@yahoo.com).*

## **Introduction**

Catalysts are important components in industrial processes [1, 2]. In using catalysts, the specificity of the catalyst is very important [3]. Nowadays, due to the high specificity of biocatalysts, their use has become common in various industries [4, 5]. The use of amylases in syrup industries and bread baking industries [6], the use of lipases in food and dairy industries [7], and the use of various types of lyases in detergent industries [8, 9] are among the cases of using biocatalysts in the industry.

However, the use of biocatalysts in industries also has limitations. One of the main limitations of using biocatalysts in the industry is their low stability *in vitro* [10, 11]. This limitation has made the use of these compounds in the industry expensive. Therefore, various methods are used to increase the stability of biocatalysts. Immobilizing the biocatalyst on a fixed substrate is one of these methods [12]. Complex formation between a biocatalyst and a chemical compound is another method in this field. Using DNA with Hemin is one of the methods of creating biocatalysts with high stability and low price. The special combination of DNA and Hemin, which has a sensor with catalytic properties, is called DNAzyme [13-15]. It has been found that the DNA with a G-quadruplex structure gives a better complex for DNAzyme formation [16, 17].

DNAzyme obtained from G-quadruplex and Hemin is used to catalyze the oxidation of 2,2-azinobis(3-ethylbenzothiazoline)-6-sulfonic acid (ABTS) by  $H_2O_2$  to form the respective colored product  $ABTS^{*+}$  [18]. In addition, this DNAzyme sensing platform has been used to detect targets from proteins of various sizes and DNA to small molecules and metal ions. Despite the widespread use of G-quadruplex-hemin DNAzyme, there is a significant challenge in its implementation [19, 20]. DNAzyme-sensor property is based on colorimetry [21]. On the other hand, Hemin's background signal is large. Therefore, it makes it difficult to use G-quadruplex-Hemin as a sensor.

One of the solutions used to eliminate this challenge is the use of carbon nanotubes. It has been determined that in the presence of single-walled carbon nanotubes, the Hemin background signal decreases [22-24]. Therefore, the sensor properties of the G-quadruplex-hemin DNAzyme are improved. However, the interaction mechanism of carbon nanotubes with G-quadruplex-hemin DNAzyme has not yet been elucidated. In this work, using molecular dynamics simulation, the interaction of G-quadruplex with hemin has been studied in the presence and absence of single-walled carbon nanotubes.

## **Experimental**

Two simulation boxes were designed. Chiral carbon nanotubes (6, 5) with a diameter of 7.46 Å and 83.1 Å length were designed and placed at the center of one simulation box. In this box, Hemin was randomly placed. In the second box, Hemin was randomly placed along with DNA. To compare the

results with available experimental data, DNA was used in G-quadruplex form. The G-quadruplex structure with the entry 1KF1 was obtained from the protein data bank [25]. Two designed simulation boxes were filled with TIP3P model water [26]. Appropriate ions were added to each box to neutralize the system. Molecular dynamics simulation calculations were performed with Gromacs software version 5.1.2 using the Amber force field ff99SB [27]. Since the Gromacs software does not have the force field parameters of the Hemin and carbon nanotube by default, these parameters were obtained from the *Ambertools* package [28, 29]. For this purpose, the Hemin and carbon nanotube structures were optimized using the density functional theory method with the basis set of 6-31G by the software GAMESS [30, 31]. To control the optimization of structures, frequency calculations at the same level were carried out using the density functional theory method, and no imaginary frequency was observed. To eliminate the bad contacts between particles in the simulation boxes, all systems are minimized in terms of energy using the steepest-descent method. In two steps, each for 10 nanoseconds at the time step of 2 fs, the systems were equilibrated in the NVT and NPT ensembles, respectively. In the final step, the molecular dynamics simulation was performed for 300 nanoseconds at a time step of 2 fs. To increase the accuracy of the simulations and to evade any dependency of results on the initial conditions, each simulation was repeated two times under different initial conditions. The control of the system temperature and pressure in all the simulation stages was performed with V-rescale and Berendsen thermostats, respectively. The chemical bond between G-quadruplex and the Hemin was bound by the LINCS algorithm [32, 33] and the chemical bonds of water molecules were bound by the SETTLE algorithm [34]. The PME algorithm was used to calculate the electrostatic interactions.

#### *Techniques and software used*

Gromacs V. 5.1.2 for molecular dynamics

GAMESS for quantum calculations

### **Results and discussion**

In Figure 1, the structure of G-quadruplex, DNA, and CNT is shown.

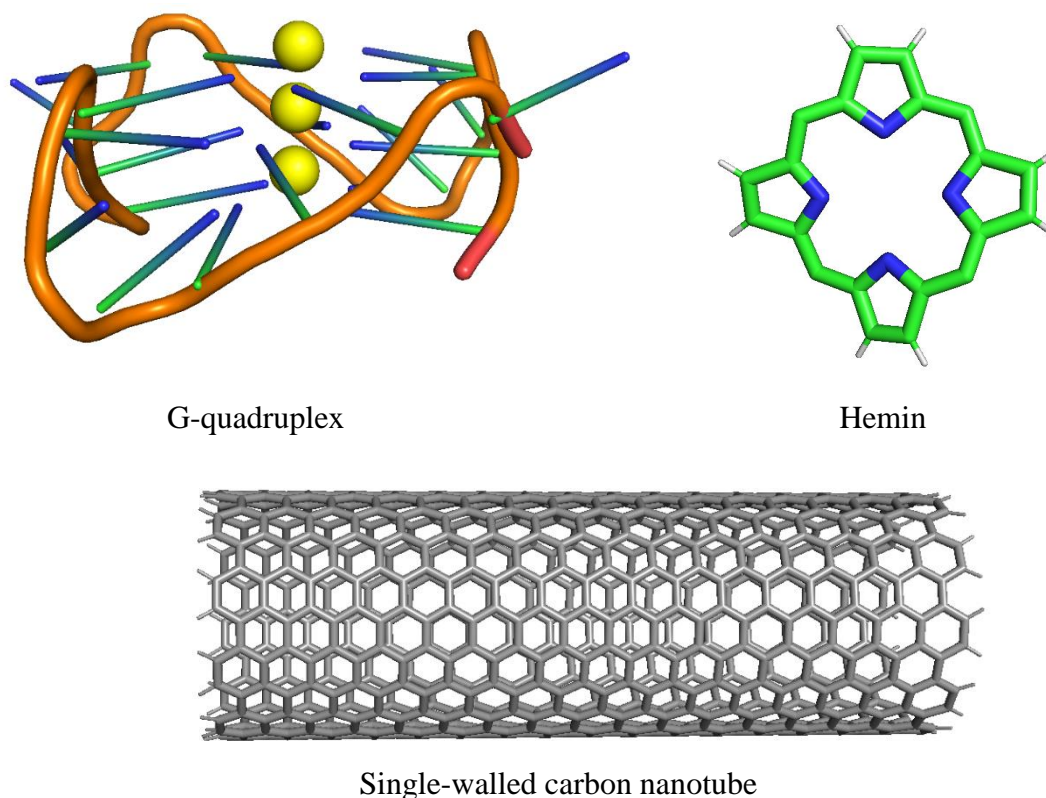


**Figure 1.** The structure of compounds studied in this work.

The sampling of the suitable sample from molecular trajectory for analysis has always been one of the issues which are interested in molecular dynamics simulation. The sampling of the averaging of the end several time steps in the simulation or sampling of the averaging of the several nanoseconds in equilibrium condition is among these methods. In these methods, variations of a quantity such as root-mean-square deviation or radius of gyration are used. But there is no physical concept in the average of atomic coordinates. So, for the sampling of the simulations, the free energy landscape (FEL) analysis method is used. Calculations of the root-mean-square-deviation (RMSD) and the G-quadruplex's radius of gyration (Rg), obtaining the possibility of the presence of G-quadruplex configuration in every corresponding value of RMSD and Rg and calculation of the free energy of configurations based on the probability values of presence are the three main stages of FEL analysis[35]. RMSD values (nm) and Rg value of G-quadruplex for the studied system during simulation time (ns) are shown in Figure 2. The Root Mean Square Deviation (RMSD) is obtained from the following equation:

$$\text{RMSD}(t_1, t_2) = \left[ \frac{1}{M} \sum_{i=1}^N m_i \|r_i(t_1) - r_i(t_2)\|^2 \right]^{1/2} \quad (1)$$

Where  $r_i$  is the atom position at time  $t$  and  $M = \sum_{i=1}^N m_i$ .

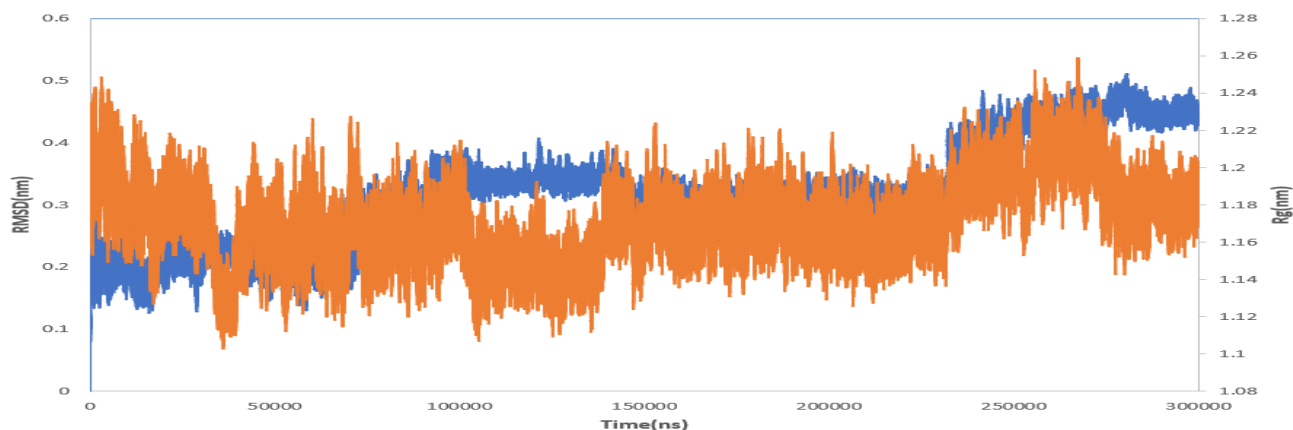
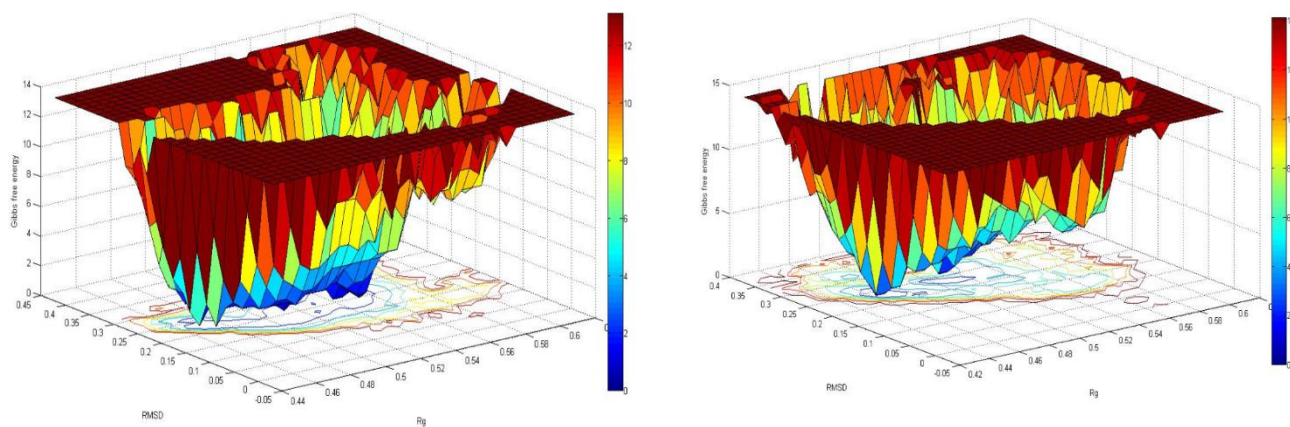


**Figure 2.** root-mean-square deviation (blue) and radius of gyration (orange) of G-quadruplex versus simulation time

According to Figure 2, RMSD changes are in the range of 0.1 to 0.5 nm. This range of variation is not large considering the size of the G-quadruplex. Therefore, it shows that the simulation time is appropriate. The changes in Rg, which is a measure of the size of the G-quadruplex, show that the G-quadruplex has not changed much. Based on these quantities, the free energy diagram of the studied systems was obtained. The results are shown in Figure 3.



G-quadruplex-Hemin-CNT

G-quadruplex-Hemin

**Figure 3.** Free Energy Landscape of the simulated system.

According to this figure, the appropriate structure was sampled from the performed simulations. To investigate the effect of carbon nanotube on the affinity of Hemin interaction with the G-quadruplex, the distance between the center of mass of these two molecules was calculated in the presence and absence of the nanotube. The result was shown in Figure 4.



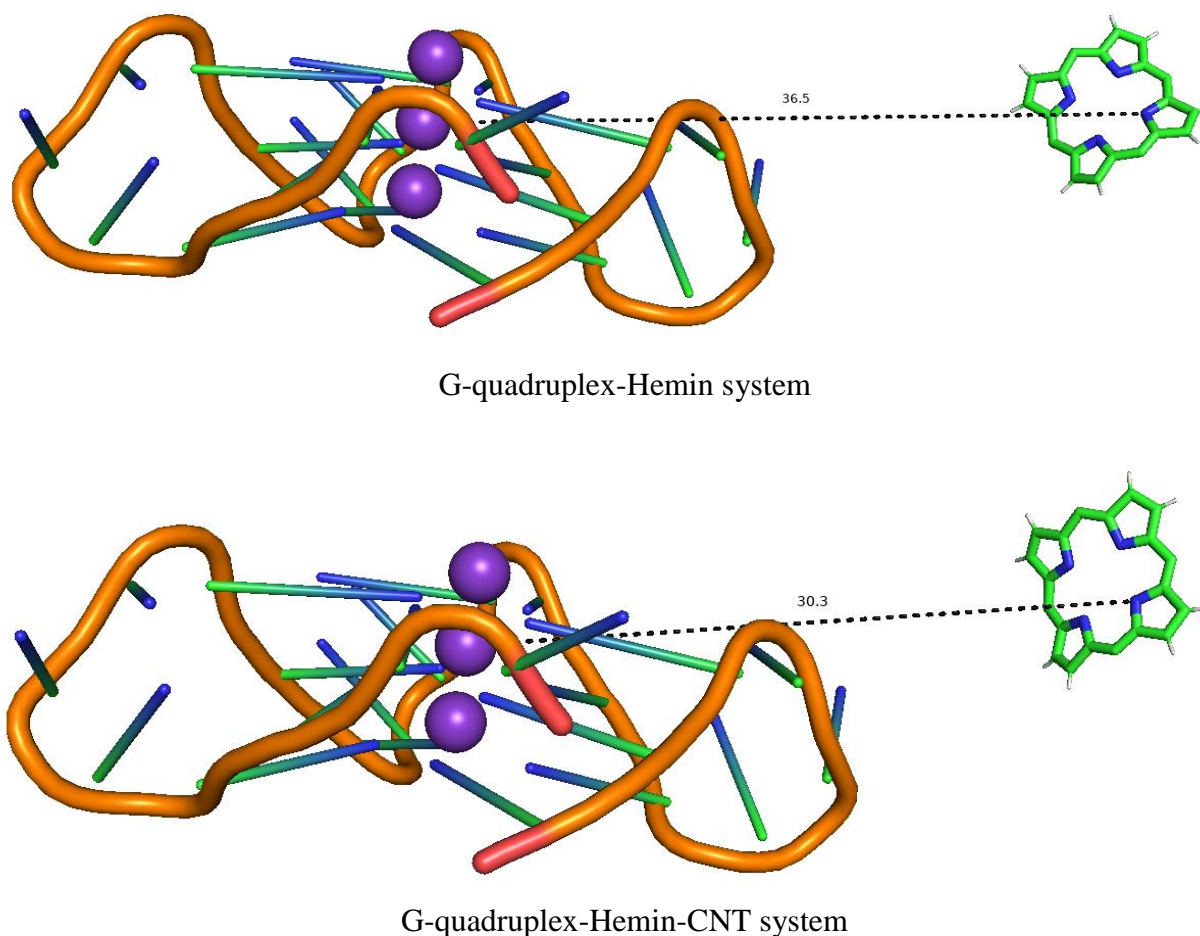


**Figure 4.** The distance between the center of mass of G-quadruplex and Hemin in the simulated systems in angstroms.

The figure shows that the nanotube has caused the distance between G-quadruplex and Hemin to decrease. It means that the nanotube has increased the affinity of binding of Hemin to G-quadruplex. Increasing Hemin to G-quadruplex affinity can reduce the background signal and improve complex sensory performance. To investigate the mechanism of increasing binding affinity more closely, the conformational factor denoted as  $P_i$ , was calculated. For this purpose, the model developed by Housainidokht et al., in which  $P_i$  is considered to be the affinity, was used[36].  $P_i$  is the contacts mean with a certain residue over the simulation time, which can be obtained from the equation  $P = \frac{n_i}{\langle N \rangle}$ .  $\langle N \rangle$  is obtained from equation (2).

$$\langle N \rangle = \sum_{i=1}^N \frac{n_i}{N} \quad (2)$$

Where,  $n_i$  is the number of contacts with the residue  $i$ , and  $N$  is the number of residues in the G-quadruplex structure. The  $P_i$  conformation factor, when greater than 1, represents high amounts of affinity for the ligand, and it can be seen that the residues with  $P_i > 1$  are used as binding sites. The calculated values of the conformational factor are listed in Table 1.

**Table 1.** conformational factor of G-quadruplex residue

Residue	Absence of CNT	Presence of CNT
1	0.03	2.03
2	0.48	1.99
3	0.65	0.88
4	0.78	0.99
5	0.05	4.48
6	1.66	2.66
7	1.09	1.98
8	0.99	5.58
9	0.00	0.66
10	0.00	1.11
11	0.00	1.89
12	0.00	8.84
13	0.00	6.67
14	0.35	3.36
15	0.01	0.58
16	0.00	0.36
17	0.00	0.39
18	0.11	0.65
19	0.05	0.99
20	0.00	0.84
21	0.00	0.69
22	0.11	0.48

According to the table, it can be seen that the nanotube has significantly affected the conformational factor. So, in the presence of nanotubes, the conformational factor of G-quadruplex residues has increased. This increase in conformational factor is observed mostly in the middle and initial residues of the G-quadruplex. In other words, Hemin has interacted with the quadruplex from the top and side. These results are consistent with the experimental results that show the improvement of DNAzyme sensor properties in the presence of nanotubes [37-39].

## **Conclusion**

Since biological sensors are far more efficient than chemical sensors, many efforts are being made to develop these sensors. However, there is an important limitation in the application of biosensors *in vitro*, which is related to the instability of the biosensor in these conditions. The system including G-quadruplex, Hemin and carbon nanotube is one of the proposed solutions for this problem. Many industries such as food contamination detection, pathogen detection and metal ion detection are industries that use this system as a sensor. However, the stabilization mechanism of the biosensor in the presence of carbon nanotubes is not well understood. DNAzyme-sensor property is based on colorimetry and hemin's background signal is large. Therefore, it makes it difficult to use G-quadruplex-Hemin as a sensor. In this work, molecular dynamics simulation method is used to understand the role of carbon nanotube in this stability. The calculation of the interaction parameters showed that the carbon nanotube reduce the hemin's background signal and stabilizes the sensor system by increasing the binding affinity of Hemin to the G-quadruplex.

## **References**

1. Torabi S, Jamshidi M, Amooshahi P, Mehrdadian M, Khazalpour S. Transition metal-catalyzed electrochemical processes for C–C bond formation. *New Journal of Chemistry*. 2020;44(36):15321-36.
2. Parshall GW, Putscher RE. Organometallic chemistry and catalysis in industry. *Journal of Chemical Education*. 1986;63(3):189.
3. Keatinge-Clay AT, Shelat AA, Savage DF, Tsai S-C, Miercke LJ, O'Connell III JD, et al. Catalysis, specificity, and ACP docking site of *Streptomyces coelicolor* malonyl-CoA: ACP transacylase. *Structure*. 2003;11(2):147-54.
4. Hughes G, Lewis JC. Introduction: biocatalysis in industry. 2018;118(1):1-3.
5. Pyser JB, Chakrabarty S, Romero EO, Narayan AR. State-of-the-art biocatalysis. *ACS Central Science*. 2021;7(7):1105-16.
6. Souza PMd, Magalhães PdO. Application of microbial  $\alpha$ -amylase in industry-A review. *Brazilian journal of microbiology*. 2010;41:850-61.
7. Ray A. Application of lipase in industry. *Asian Journal of Pharmacy and technology*. 2012;2(2):33-7.
8. Kirk O, Borchert TV, Fuglsang CC. Industrial enzyme applications. *Current opinion in biotechnology*. 2002;13(4):345-51.
9. Bell EL, Finnigan W, France SP, Green AP, Hayes MA, Hepworth LJ, et al. Biocatalysis. *Nature Reviews Methods Primers*. 2021;1(1):1-21.



10. Kazlauskas RJ. Molecular modeling and biocatalysis: explanations, predictions, limitations, and opportunities. *Current opinion in chemical biology*. 2000;4(1):81-8.
11. Sheldon RA, Brady D. The limits to biocatalysis: pushing the envelope. *Chemical Communications*. 2018;54(48):6088-104.
12. Morshed MN, Behary N, Bouazizi N, Guan J, Nierstrasz VA. An overview on biocatalysts immobilization on textiles: Preparation, progress and application in wastewater treatment. *Chemosphere*. 2021;279:130481.
13. Willner I, Shlyahovsky B, Zayats M, Willner B. DNAzymes for sensing, nanobiotechnology and logic gate applications. *Chemical Society Reviews*. 2008;37(6):1153-65.
14. McConnell EM, Cozma I, Mou Q, Brennan JD, Lu Y, Li Y. Biosensing with DNAzymes. *Chemical Society Reviews*. 2021.
15. Zhao M, Wang M, Zhang X, Zhu Y, Cao J, She Y, et al. Recognition elements based on the molecular biological techniques for detecting pesticides in food: a review. *Critical Reviews in Food Science and Nutrition*. 2021:1-24.
16. Dong J, O'Hagan MP, Willner I. Switchable and dynamic G-quadruplexes and their applications. *Chemical Society Reviews*. 2022.
17. Yang H, Zhou Y, Liu J. G-quadruplex DNA for construction of biosensors. *TrAC Trends in Analytical Chemistry*. 2020;132:116060.
18. Liu J, Cao Z, Lu Y. Functional nucleic acid sensors. *Chemical reviews*. 2009;109(5):1948-98.
19. Kong D-M, Xu J, Shen H-X. Positive effects of ATP on G-quadruplex-hemin DNAzyme-mediated reactions. *Analytical chemistry*. 2010;82(14):6148-53.
20. Stadlbauer P, Islam B, Otyepka M, Chen J, Monchaud D, Zhou J, et al. Insights into G-Quadruplex–Hemin Dynamics Using Atomistic Simulations: Implications for Reactivity and Folding. *Journal of Chemical Theory and Computation*. 2021;17(3):1883-99.
21. Li D, Ling S, Cheng X, Yang Z, Lv B. Development of a DNAzyme-based colorimetric biosensor assay for dual detection of Cd<sup>2+</sup> and Hg<sup>2+</sup>. *Analytical and Bioanalytical Chemistry*. 2021;413(28):7081-91.
22. Britz DA, Khlobystov AN. Noncovalent interactions of molecules with single walled carbon nanotubes. *Chemical Society Reviews*. 2006;35(7):637-59.
23. Khan S, Burciu B, Filipe CD, Li Y, Dellinger K, Didar TF. DNAzyme-based biosensors: Immobilization strategies, applications, and future prospective. *ACS Nano*. 2021;15(9):13943-69.

24. Wang H, Zhang F, Wang Y, Shi F, Luo Q, Zheng S, et al. DNzyme-Amplified Electrochemical Biosensor Coupled with pH Meter for Ca<sup>2+</sup> Determination at Variable pH Environments. *Nanomaterials*. 2021;12(1):4.
25. Parkinson GN, Lee MP, Neidle S. Crystal structure of parallel quadruplexes from human telomeric DNA. *Nature*. 2002;417(6891):876-80.
26. Price DJ, Brooks III CL. A modified TIP3P water potential for simulation with Ewald summation. *The Journal of chemical physics*. 2004;121(20):10096-103.
27. Van Der Spoel D, Lindahl E, Hess B, Groenhof G, Mark AE, Berendsen HJ. GROMACS: fast, flexible, and free. *Journal of computational chemistry*. 2005;26(16):1701-18.
28. Macke TJ, Svrcek-Seiler W, Brown RA, Kolossváry I, Bomble YJ, Case DA, et al. *AmberTools Users' Manual*. Ver; 2010.
29. Bazoobandi M, Bozorgmehr MR, Mahmoudi A, Morsali A. The Effect of Temperature on the Interaction of Phenanthroline-based Ligands with G-quadruplex: In Silico Viewpoint. *Combinatorial Chemistry & High Throughput Screening*. 2019;22(8):546-54.
30. Gordon MS, Schmidt MW. Advances in electronic structure theory: GAMESS a decade later. *Theory and applications of computational chemistry*: Elsevier; 2005. p. 1167-89.
31. Imbalzano G, Zhuang Y, Kapil V, Rossi K, Engel EA, Grasselli F, et al. Uncertainty estimation for molecular dynamics and sampling. *The Journal of Chemical Physics*. 2021;154(7):074102.
32. Hess B, Bekker H, Berendsen HJ, Fraaije JG. LINCS: a linear constraint solver for molecular simulations. *Journal of computational chemistry*. 1997;18(12):1463-72.
33. Nabavi M, Housaindokht MR, Bozorgmehr MR, Sadeghi A. Theoretical design and experimental study of new aptamers with the enhanced binding affinity relying on colorimetric assay for tetracycline detection. *Journal of Molecular Liquids*. 2022;349:118196.
34. Miyamoto S, Kollman PA. Settle: An analytical version of the SHAKE and RATTLE algorithm for rigid water models. *Journal of computational chemistry*. 1992;13(8):952-62.
35. Sargsyan K, Grauffel C, Lim C. How molecular size impacts RMSD applications in molecular dynamics simulations. *Journal of chemical theory and computation*. 2017;13(4):1518-24.
36. Housaindokht MR, Bozorgmehr MR, Bahrololoom M. Analysis of ligand binding to proteins using molecular dynamics simulations. *Journal of theoretical biology*. 2008;254(2):294-300.
37. Zhang Y, Li B. Reducing background signal of G-quadruplex–hemin DNzyme sensing platform by single-walled carbon nanotubes. *Biosensors and Bioelectronics*. 2011;27(1):137-40.

38. Li D, Li C, Liang A, Jiang Z. SERS and fluorescence dual-mode sensing trace hemin and K<sup>+</sup> based on G-quarplex/hemin DNzyme catalytic amplification. *Sensors and Actuators B: Chemical*. 2019;297:126799.
39. Selvaraj C, BTV S, Xiong H. *Developing Trends in DNA Biosensor and Their Applications. Metal, Metal-Oxides and Metal Sulfides for Batteries, Fuel Cells, Solar Cells, Photocatalysis and Health Sensors*: Springer; 2021. p. 245-84.